The effect of hydrocarbon pollution on polysulfone-based membranes in aqueous separations

Kristianne Tempelman[1], Serena Casanova[1,a], Nieck E. Benes[1]*

[1]Film in Fluids, University of Twente, Department of Science and Technology, MESA+ Institute for Nanotechnology, P.O. Box 217, 7500 AE Enschede, The Netherlands

[a]Present address: Department of Chemical Engineering and Centre for Advanced Separations Engineering, University of Bath, Bath BA26AH, U.K..

** Corresponding author: n.e.benes@utwente.nl*

Abstract

This work investigates the influence of hydrocarbon pollution on the performance of desalination membranes with a polysulfone support. Toluene was chosen as the model hydrocarbon compound and permeation measurements were performed on two commercial membranes with a polysulfone support in water saturated with toluene. Over time, the TriSep TS80 membrane under analysis broke down and the delamination of the separation layer was observed. The influence of the polysulfone layer on the membrane deterioration was studied in detail by the use of a model system of a thin polysulfone film on top of a silicon wafer. *In situ* spectroscopic ellipsometry, and *in situ* optical microscopy revealed that the non-ideality of the hydrocarbon in water system initiates a dewetting of the polysulfone layer which is the root cause of the membrane failure.

Keywords

Spectroscopic ellipsometry, solvent resistance, membranes, polysulfone, nanofiltration

1. Introduction

Purification of water contaminated with hydrocarbons poses a challenging problem and is required to prevent release of hydrocarbons into the environment [1–3]. In the oil and gas industry, three to four barrels of contaminated water are produced for the production of one barrel oil or gas [4]. In this case, the so-called “produced water” is a saline by-product in the recovery of oil and gas from a well [5], which needs a pretreatment in order to be released in the environment. Today, common water treatment processes

include the use of membranes. Reverse osmosis (RO) membranes and nanofiltration (NF) membranes are a well-established and energy efficient separation technique and widely applied [4,6,7]. The use of a one-step treatment using RO or NF membranes for waste water or produced water treatment would be a simple and low-cost operation [4,5,8,9]. However, at this moment, membrane fouling when in contact with the wastewater is still a large problem, limiting the membrane process efficiency and the use of RO or NF membranes in general [10–14]. Pre-treatment steps such as adsorption, gravity settling or coagulation techniques have shown to be effective in reducing the membrane fouling [15], but even after the pre-treatment step significant fouling could still be observed.

The industrial wastewater streams and produced water from the petroleum industry have been analyzed thoroughly and ~~one of components present in these water streams~~often the presence of ~~–~~organic contaminants (Total organic carbon or TOC content) is appointed as the cause for membrane fouling and degradation ~~in wastewater or produced water treatments is the presence of organic contaminants (Total organic carbon or TOC content)~~ [16,17]. The underlying phenomena of membrane fouling and degradation when in contact with TOCs is still poorly understood. It was suggested that the fouling was caused by interactions between dissolved and suspended solutes in the feed and the membrane surface, resulting in large flux declines [11]. Van der Bruggen et al. (2001) found that both the membrane surface charge and the membrane hydrophobicity play a role in the adsorption of solutes onto the membrane surface, lowering the water solubility [17,18].

NF membranes are the preferred option for the treatment of produced water, based on considerations on the trade-off between the applied operating pressure and the separation factor obtained [5], especially when the water is to be reused within the operational process [19]. On the whole, NF membranes are mostly thin film composite (TFC) membranes [20], conformation that helps limiting the operational pressure, with typically a separating layer thickness of 50-200 nm. The most commonly used selective barrier consists of a highly cross-linked (semi) aromatic polyamide layer [21]. Polyamides are known for their enhanced durability, their reasonable chemical resistance, and can effectively reject inorganic solutes [21]. TFC membranes are made by either coating or interfacial polymerization of a thin membrane on top of an ultrafiltration (UF) support, a porous asymmetrical structure that provides mechanical stability[5]. The support layer is typically made from polysulfone or polyethersulfone [20], polymers deemed as suitable thanks to their polarity and roughness that benefit adhesion to the selective layer [22]. Despite their popularity, these polymers are repeatedly reported to fail in harsh environments and when used for solvent separations [23]. The overall TFC durability is to ascribe largely to the structural stability of the

Commented [SC1]: Maybe reference R.W. Baker, Membrane Technology and Applications, 3rd ed., John Wiley & Sons. Ltd., 2012. ?

support layer, and it is therefore of great interest to understand the nature of substrate failure, to make informed decisions on the choice of membranes for specific systems.

In this work, the interaction between the dissolved hydrocarbons, the separating polyamide layer and the supporting polysulfone layer was studied. The performance of two commercial membranes, TriSep TS80 and DOW FILMTEC NF270, were compared in water/toluene mixtures. The model hydrocarbon solute was chosen due to its representative properties and because one of the most commonly separated solvents in organic solvent nanofiltration[24].The interaction between the polysulfone support and the solute was studied in further detail with *in situ* spectroscopic ellipsometry, atomic force microscopy and optical microscope monitoring using a model system ~~existing~~ consisting of a thin polysulfone layer on top of a silicon wafer in both a water, toluene and water saturated with toluene ambient.

2. Experimental

2.1. Materials

Polysulfone Udel ® P-3500 (Amoco), Cyclopentanone (ReagentPlus®, ≥99 %, Sigma-Aldrich), toluene (anhydrous, ≥ 99.8 %, Sigma-Aldrich) were used as received.

Silicon wafers (100, front side polished, CZ test grade, Silchem) were used as a substrate for the spin-coated layer. The wafers were stored under clean-room conditions until being cut. Prior to use, the wafers were cleaned with Acetone (Chromasolv® plus, for HPLC 99.9 %, Sigma-Aldrich).

The purchased commercial membranes TriSep TS80 (flat sheet, Microdyn Nadir) and DOW FILMTEC™ NF270 (flat sheet, DOW) were used for permeance measurements. Both membranes are a semi-aromatic polyamide based thin film composite membrane with a polysulfone support.

Unless otherwise stated, deionized water (18.2 MΩ cm, Milli-Q Advantage A10, Millipore) was used.

2.2. Sample preparation

Thin polysulfone films (~250 nm) were prepared on silicon wafers by spin-coating a solution of polysulfone in cyclopentanone (3wt%) using a two-step spinning program:

1. 30 s 500 rpm
2. 5 min 1000 rpm

After spin-coating, the samples were annealed in a chamber over (Carbolite HTMA 5/28) at 215 °C for 8 hours under a constant nitrogen flow (5 mL min^{-1}).

2.2.1. *Permeation measurements of TriSep TS80 and DOW NF270*

Prior to the permeance experiments, both the TriSep TS80 and DOW NF270 membranes were placed in water at least one day before the measurement, in order to remove the glycerol inside the membranes. After soaking, the membranes were rinsed with water and placed into the permeance set-up.

Permeance experiments in demineralized-water and in demineralized-water saturated with toluene were performed on a custom-built setup (Convergence, The Netherlands). All measurements were performed at a constant feed pressure of 15 bar and at a constant temperature of 25 °C, in cross-flow operation with a membrane area of 46 cm^2. Permeate fluxes were measured using an M13 mini-Coriflow Coriolis mass-flow meter (Bronkhorst, The Netherlands). For each permeance measurement, the sample was first ~~measured~~ tested in demineralized-water for at least one hour, which served as pre-compaction, before the feed was changed to water saturated with toluene at the same pressure. A water solution saturated with toluene was obtained by mixing ~4.5 L of demineralized-water with ~250 mL of toluene for at least one day. Saturation was accomplished when a thin layer of toluene remained on top of the water solution.

Commented [SC2]: I think it might make some sense to clarify here that the membranes were not pre-compacted at a p higher than 15 bar before the experiment.

After the measurement, to remove the water and prevent collapse of the pore structure, the membranes were placed in ethanol for at least 2 hours, washed with fresh ethanol and subsequently placed in hexane for at least 2 hours. The membranes were then washed with fresh hexane and dried to the air.

Scanning electron micrographs of the membranes used for permeation experiments were taken with a JEOL JSM-7610 field emission scanning electron microscope (FE-SEM). Samples were coated with a 10 nm chromium layer (Quorum Q150T ES) prior to imaging. Cross-section samples were cut after immersing in liquid nitrogen.

2.3. Characterization

2.3.1. *In situ spectroscopic ellipsometry*

In situ swelling experiments were performed with spectroscopic ellipsometry using an alpha-SE from J.A. Woollam Co., in combination with a custom-built glass cell (V = 100 mL) with quartz windows with an incident angle of 70°. The cell temperature was controlled with an external water-bath (LAUDA-Brinkmann, LP.), allowing water to flow through the outer walls of the cell. An external temperature

control, with a temperature sensor inside the cell was used for temperature control. To correct for the optical retardance of the quartz windows, a calibration with a 60 nm SiO_2 wafer was performed prior to each measurement.

Prior to each *in situ* swelling measurement, the polymer sample was measured outside the cell, inside the cell and then the *in situ* measurement was started. After 2 minutes dry, 70 mL of the temperature calibrated liquid (water or toluene) was poured into the cell. For the measurement in water saturated with toluene solution, water was first poured into the cell and on top of the water, a small amount of toluene (~2 mL) was carefully added. In this case, the toluene slowly diffuses into the water until the maximum solubility limit is reached. The maximum solubility of toluene in water at 25 °C is in average 547 ± 8.5 ppm [25].

The data was modelled using the CompleteEase software package (J.A. Woollam Co.) and in the wavelength range of 370-900 nm. The silicon substrate was modelled using the built-in optical properties of a silicon wafer, on top of which a 2 nm native oxide layer was modelled. The model-generated data is fitted numerically to the measured spectrum and the fit quality is quantified by the root mean square error (MSE) between the measured and the generated spectra. For the majority of Cauchy-type thin (up to 500 nm) polymer films deposited on silicon wafers, MSE values representing very good fits are in the range 1-5. For thicker films values of 10-20 are acceptable. The thickness and refractive index of the polysulfone film was modelled using a Cauchy dispersion[26] with the thickness, *A*, *B* and *C* as fit parameters. An ambient was added to the model based on the Cauchy dispersion of the solvent. The optical dispersion of water, toluene and water-toluene was determined by measuring the refractive index at 7 different wavelengths (365.0 nm, 400.0 nm, 450.0 nm, 500.0 nm, 590.0 nm, 700.0 nm, 800.0 nm) using a digital multiple wavelength refractometer (Schmidt Haensch ATR-L) at 22 °C. The determined Cauchy constants of each solvent are provided in the Supplementary Information.

The swelling degree of a polymer film upon swelling was calculated using Eq.1.

$$SD = \left(\frac{d_{\mathrm{swollen}}}{d_{\mathrm{dry}}} - 1\right) \cdot 100\% \qquad [1]$$

Where SD is the swelling degree, and d_{dry} and d_{swollen} are the dry and swollen thickness of the film, respectively.

The normalized refractive index upon swelling in solvents was calculated using Eq.2.

$$n_{\mathrm{norm}} = \frac{n_{\mathrm{swollen}} - n_{\mathrm{solvent}}}{n_{\mathrm{dry}} - n_{\mathrm{solvent}}} \quad [2]$$

Where n_{norm} is the normalized refractive index, n_{dry} is the refractive index of the non-swollen polymer film, n_{swollen} is the refractive index of the swollen polymer film in a solvent, and n_{solvent} is the refractive index of the pure solvent.

2.3.2. *Optical microscopy*

An inverted optical microscope (Zeiss Axiovert 40 MAT microscope) in combination with a Hamamatsu ORCA-Flash4.0 LT camera was used to image the swelling of a spin-coated polysulfone film in toluene and in water saturated with toluene as function of time. The sample was placed topside down in a transparent flask filled with the solvent, using a 1 mm thick spacer between the bottom of the flask and the sample. Images were taken at a ten minutes interval at 20x magnification.

2.3.3. *Atomic Force Microscopy*

Spin-coated polysulfone samples that were immersed in water satured in toluene for 8 and 24 hours, or immersed in pure toluene for 24 hours and a dry polysulfone sample were used for Atomic Force Microscopy (AFM) measurements. After solvent exposure, the samples were dried in a vacuum oven at 50 °C for 4 hours. AFM measurements were performed with Multimode 8 AFM (Bruker) with a NanoScope V controller and a JV vertical engage scanner in tapping mode at room temperature. A silicon cantilever (model NCH, Nanoworld, Switzerland), with a resonance frequency of 320 kHz, a force constant of 42 N m^{-1} and a polygon-based pyramid shape with a tip radius of 8 nm was used. The samples were scanned at a rate of 1 Hz. The NanoScope software (version 8.15) was used for image processing and analysis.

3. Results and Discussion

3.1. Permeation measurements

Figure 1~~Figure 1~~ shows the permeation results of the commercial TriSep TS80 in demineralized water, followed by water saturated with toluene at a constant pressure of 15 bar. The water permeance for the TriSep TS80 is ~4 L m^{-2} h^{-1} bar^{-1}. Upon the introduction of the water-toluene solution, the permeance decreases immediately within the first 15 minutes to ~3 L m^{-2} h^{-1} bar^{-1}, after which a sharp progressive increase with time is observed. This sharp progressive increase with time as observed for the water-toluene permeance, indicates a breakdown of the membrane.

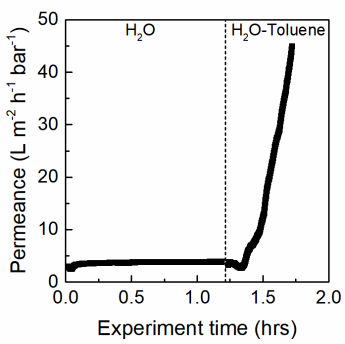

Figure 1 – The permeance (left axis) of a commercial TriSep TS80 nanofiltration membrane at a constant pressure of 15 bar. The first 1.2 hours shows the permeance of demineralized water. At 1.2 hours a saturated solution of water with toluene was introduced.

A similar experiment as done for the TriSep TS80 membrane was performed for the commercial DOW NF270 membrane, also a nanofiltration membrane. For the DOW NF270 membrane a constant decline in the H_2O-toluene permeance was observed over a period of six days as is shown in Figure 2~~Figure 2~~. The initial decline from ~12 L m^{-2} h^{-1} bar^{-1} to ~7 L m^{-2} h^{-1} bar^{-1} can be attributed to the introduction of toluene, as also observed in literature [17]. The slower decline over time was attributed to membrane fouling[27] due to pollution (see Figure S1 in Supporting Information) and is caused by contamination present in the set-up itself. As this phenomena was also observed in the pure water permeance measurement (Figure S1 in Supporting Information), its relevance in the context of our observations is minimal, as the fouling behaviour of the membranes under analysis is beyond the scope of this work.

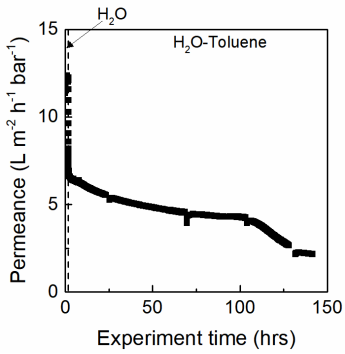

Figure 2 – The permeance (left axis) of a commercial DOW NF270 nanofiltration membrane at a constant pressure of 15 bar. The first 1 hour shows the permeance of demineralized water. At ~1 hour a saturated solution of water with toluene was introduced.

Although both TriSep TS80 and DOW NF270 are semi-aromatic polyamide-based membranes on a polysulfone support, their performance in water saturated with toluene was observed to be entirely different. In previous studies it was shown that with an increased hydrophobicity of the membrane, an increasedinteraction with the organic solute was obtained. As a result, the performance of the membrane decreased with increasing hydrophobicity of the membrane [17]. The hydrophobicity of both TriSep TS80 and DOW NF270 have already been studied widely in literature and the reports on the contact angles vary from 15° to 43° for DOW NF270 [12,19,28,29] and from 48° to 57° for TriSep TS80 [28–30]. In general, TriSep TS80 was always found to be less hydrophillic compared to DOW NF270. The higher hydrophobicity of the TriSep TS80 membrane compared to the DOW NF270, explained the stronger effect of the presence of toluene on the membrane performance of the TriSep TS80 membrane. Other than the hydrophobicity of the two commercial membranes, also the membrane structure was studied using scanning electron microscopy (SEM).

In Figure 3~~Figure 3~~ the cross-section and top view SEM images of the TriSep TS80 (A,C,E,G) and DOW NF270 membrane (B,D,F,H) are displayed for a virgin membrane (A-D) and the membrane used for H_2O-toluene permeation (E-H). A clear difference in structure between the TriSep TS80 and the DOW NF270 was observed. The TriSep TS80 has a high roughness and the separation layer is approximately 260 nm thick. The interfacial polymerization layer appears to be formed on top of the polysulfone support and little interconnection between the polysulfone support and the polyamide layer is visible. The DOW NF270 on the other hand shows a smooth layer with a low macroscopic roughness with a separating layer of approximately 40 nm thick.

Upon exposure to a saturated mixture of water with toluene at 15 bar, the separating layer for the TriSep TS80 has delaminated from the polysulfone support (Figure 3~~Figure 3~~C). On the surface (Figure 3~~Figure 3~~G) a collapse of the interfacial polymerization structure could be observed. Most likely caused by the observed limited swelling of the selective layer in toluene, followed by a collapse of the structure under pressure and change in morphology upon drying. For the DOW NF270, contamination is present on the surface, confirming that the decay in permeance over a long time is the result of fouling due to pollution present in the feed. Other than the pollution, no significant changes in structure were observed.

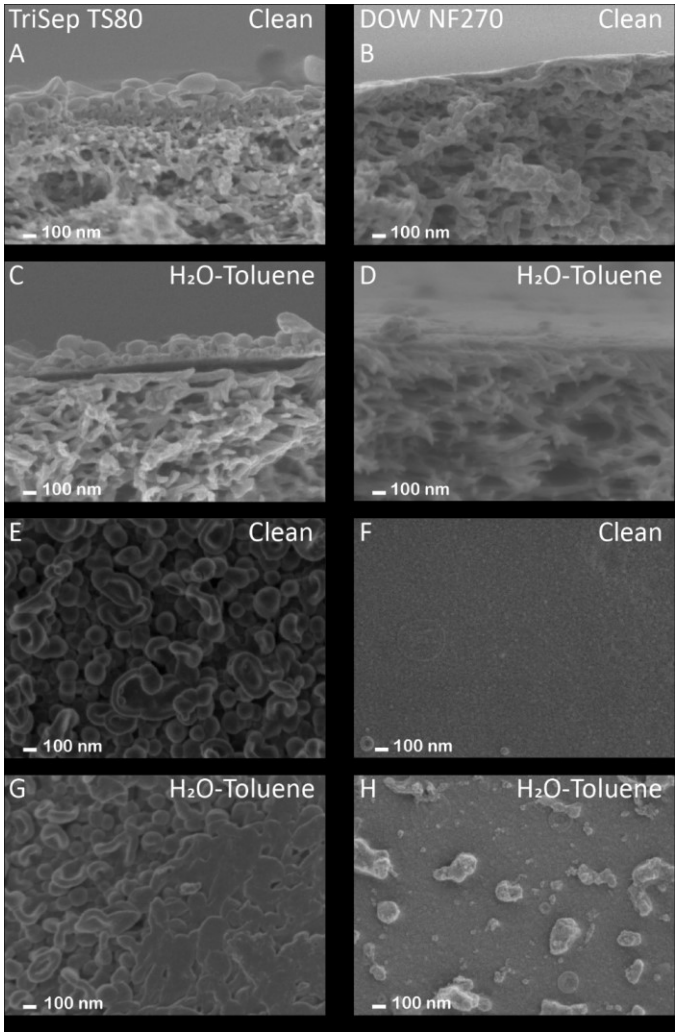

Figure 3 – FE-SEM at 50000x magnification cross-section (A-D) and top-view (E-H) images of TriSep TS80 (A,C,E,G) and DOW NF270 (B,D,F,H) of a clean non-used membrane (A,B and E,F) and when exposed to water saturated with toluene (C,D and G,H).

3.2. In situ spectroscopic ellipsometry

As polyamide layers are known to have a good chemical resistance to organic solvents [31] and the polysulfone is prone to swelling in organic solvents [32], the swelling behavior of the polysulfone support

in a water-hydrocarbon mixture was the main focus of this study. To investigate the effect of the polysulfone layer on the separation performance of a polysulfone based membrane in water polluted with hydrocarbons in detail, a model system was designed. The model system consists of a spin-coated polysulfone film on top a silicon wafer which was investigated with *in situ* spectroscopic ellipsometry.

In Figure 4~~Figure 4~~ the swelling degree and normalized refractive index as function of the experiment time are shown for polysulfone in MilliQ water, pure toluene and water saturated with toluene. No significant swelling was observed for the polysulfone layer in water, while a swelling degree of almost 80 % was obtained in toluene. The small but steady decrease in thickness with increasing experiment time indicates a slow dissolution process is taking place. In the water-toluene solution, with increasing experiment time, an excessive swelling occurs. For longer experiments times (>1000 min), the fitting error increases to such an extent that a fit of the raw data is no longer possible. This indicates a change in the sample which cannot be captured by the optical model.

In Figure 5~~Figure 5~~ the raw Ψ-data as measured for the water-toluene solution is shown. The Ψ-data is based on the p-and s-reflectivities of the bare substrate and the polymer film in an ambient. It is shown that at *t*=1252 min, the Ψ-data has collapsed onto the so-called optical envelope, which represents the substrate. The oscillatory pattern that is observed in the Ψ-data represents the transparent polysulfone film and is the result of the interference of the thin film with the light. From Figure 5~~Figure 5~~ it can therefore be concluded that the polysulfone has been removed from the substrate. In contradiction to a polysulfone film in pure toluene, the polysulfone film in water saturated with toluene first shows excessive swelling and then it appears to be removed as a whole from the substrate, no evidence of a continuous dissolution process such as was observed for polysulfone in pure toluene, was detected in water saturated with toluene.

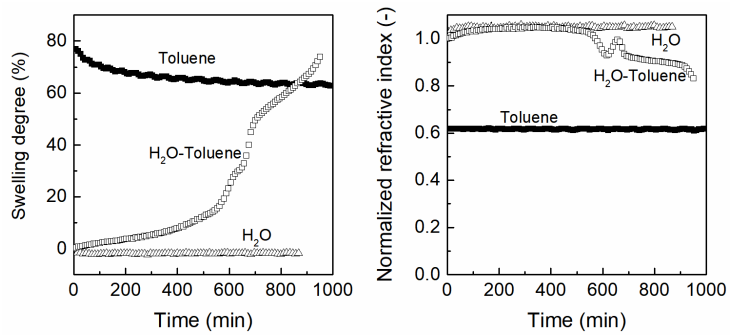

Figure 4 – *In situ* spectroscopic ellipsometry data as function of the experiment time for 230 nm polysulfone film on a silicon wafer. Swelling degree (Left) and the normalized refractive index (Right) of polysulfone in MilliQ water, pure toluene and water saturated with toluene.

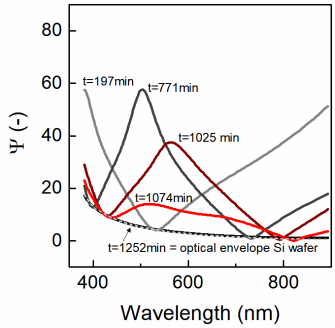

Figure 5 – Ψ-spectra for a polysulfone film on top of a silicon wafer in an ambient of water saturated with toluene as recorded during the *in situ* measurement. The oscillatory pattern indicates the presence of the polymer film. With increasing experiment time, the polysulfone film is being removed from the substrate. At *t* = 1252 min, the Ψ-signal collapsed onto the so-called optical envelope of the silicon wafer (dashed line).

3.3. Dewetting effect

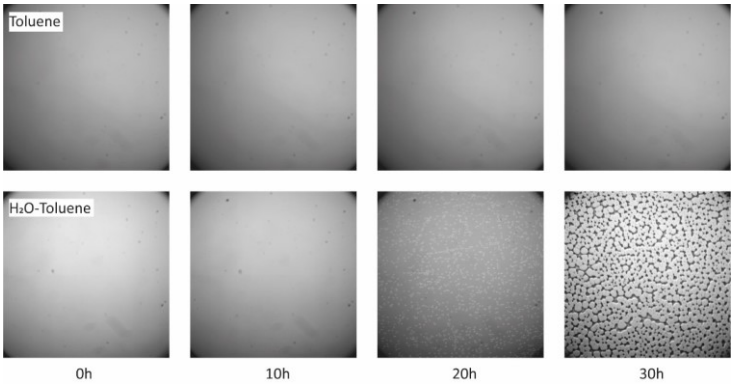

Figure 6 – *In situ* optical microscopy images of a ~200 nm film on top of a Si wafer initially and at 10, 20 and 30 hours in toluene (Top row). Bottom row shows a ~200 nm film on top of a Si wafer initially and at 10, 20 and 30 hours in water saturated with toluene. Here a dewetting mechanism was observed.

For both the TriSep TS80 membrane and the polysulfone layer on top of the silicon wafer, a similar delamination process was observed. Indicating that the non-ideality of the water-toluene solution induces a separation between the substrate and the polysulfone layer. This hypothesis is further confirmed by the optical microscopy results shown in Figure 6~~Figure 6~~. Figure 6~~Figure 6~~ shows the *in situ* progression of a ~200 nm thick polysulfone film on top of a silicon wafer in toluene (top) and water saturated with toluene (bottom) using optical microscopy. In toluene no changes were observed over the course of time. In the water-toluene solution however, small holes start to appear around 16-20 hours, which merge and eventually result in an almost complete removal of the polysulfone film around 30 hours. In order to confirm the observations in Figure 6~~Figure 6~~, atomic force microscopy (AFM) measurements have been performed. A non-swollen spin-coated polysulfone film was compared to a polysulfone film immersed in water saturated with toluene for 8 hours and 24 hours and to a polysulfone film immersed in pure toluene for 24 hours (Figure 7). A neat polysulfone film has a roughness of 0.36 ± 0.03 nm and immersion in solvent increases the roughness of the film. In Figure 7 it is shown that small holes on the surface are already present at an 8 hours exposure in a water-toluene mixture and they grow with longer immersion times. Also, for polysulfone exposed to pure liquid toluene for 24 hours, small holes could be detected.

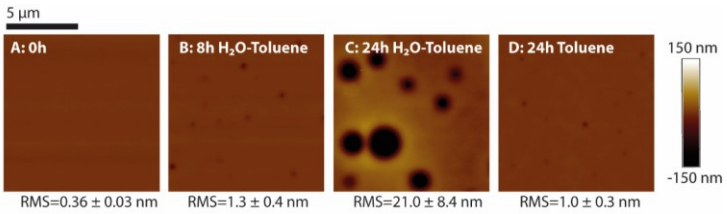

Figure 7 – AFM images of spin-coated polysulfone films without solvent exposure (A), 8 hours immersion in water oversaturared with toluene (B), 24 hours immersion in water oversaturared with toluene (C) and 24 hours immersion in toluene (D). The roughness of the film increases with the immersion time. For polysulfone in pure toluene, also holes are visible, indicating some dewetting. The error margin displays a 95% confidence interval based on 9 3x3 µm spots on the surface.

The removal of the polysulfone film from the silicon wafer is similar to the commonly observed dewetting process. When a liquid is placed on top of a non-wettable surface, it will flow and dewetting occurs. A similar process is often observed for coated glassy polymers on top of a silicon wafer when heated to temperatures above the glass transition temperature, T_g. Above the glass transition temperature, the polymer becomes liquid and has gained sufficient mobility to dewet the surface. This is known as thermal dewetting. Dewetting can also be induced by the exposure of a thin polymer film to a penetrant, known as solvent dewetting. When the penetrant is able to sufficiently dilute the polymer matrix, the glass transition temperature is decreased and an increase in the mobility of the polymer film can be observed. The stability of a polymer film on top of a substrate is either defined as stable, metastable or unstable. In case of a stable film, the film is in the lowest energy state. For a metastable film, a potential barrier has to be overcome to reach the lowest energy state. Unstable films dewet immediately. Both metastable and unstable films can dewet via nucleation, known as heterogeneous dewetting or via spinodal dewetting, also known as homogeneous nucleation.[33]

As shown with the *in situ* spectroscopic ellipsometry measurement, polysulfone swells up to 80% more than its initial thickness in pure toluene. Based on the almost instant diffusion of toluene into the polysulfone matrix and the high solvent content inside the polymer matrix, one can assume that the presence of the solvent has sufficiently depressed the glass transition temperature to around the measurement temperature [34]. For this reason, at very long immersion times (>24 hours) of the polysulfone to toluene, dewetting could be observed (Figure 7D). In this case however, the dewetting rate is much slower compared to the dewetting in water-toluene mixtures.

For polysulfone in water saturated with toluene, the dewetting rate is much faster compared to the dewetting as observed in pure toluene. In the case of water saturated with toluene, the water to toluene ratio is very large and as a result, when polysulfone swells the polysulfone, water will tag along. As the affinity between water and polysulfone is lower than the affinity of water for the silicon substrate [35,36], a thin water film is formed between the substrate and the polymer film, resulting in the dewetting of the polysulfone film.

In order to inhibit dewetting of the polymer film, several approaches can be used [33]. Chemical surface modification can be used to increase the substrate surface energy or surface tension. Cross-linking of the polymer can be used to fixate the polymer chains and to decrease the mobility of the polymer. For polysulfone it has been shown before that cross-linking using UV-radiation works to immobilize the polymer and to reduce swelling in order to prevent dewetting [37]. A different approach to prevent dewetting is by adding nanofillers in the polymer, changing the interfacial interactions.

3.4. Membrane dewetting

The dewetting as observed for the model system of a thin polysulfone layer on top of a silicon support can be used to explain the membrane performance of the TriSep TS80 and DOW NF270 membranes. For the membranes, the polyamide top layer can be considered as the comparable layer to the silicon substrate. The dewetting as observed in the model system can be compared with the NF membranes, as the high chemical resistance of the polyamide and limited swelling of the polyamide suggests a low affinity of the polyamide towards toluene. In both cases there is a high availability of water for which sorption in either of the polymers is unfavourable and which will over time accumulate at the interface between the different polymer layers.

As shown in section 3.1, the commercial TriSep TS80 membrane shows a dewetting of the interfacial polymerization layer from the polysulfone substrate upon exposure to a water solution saturated with toluene. The commercial DOW NF270 membrane however, shows no such dewetting and remains stable over the timespan of six days. The main reason for this contradiction in behavior between these two membranes is the integration of the interfacial polymerization layer into the polysulfone support and the hydrophobicity of the membranes. The IP layer of the TriSep TS80 is formed on top of the polysulfone support and the growth of the film has occurred in the organic phase as shown by the lobs on top of the membrane. In case of the DOW NF270 membrane, the IP layer is significantly thinner than for the TriSep TS80 membrane and it seems to be better integrated into the polysulfone support. The higher

hydrophobicity of the TriSep TS80 membranes caused that more toluene was able to diffuse through the polyamide layer and swell the polysulfone support. Because of the high availability of water, for which the affinity for the swollen polysulfone is extremely low, a thin water film can be formed between the polyamide separating layer and polysulfone support resulting in the delamination of the polyamide layer. In order to increase the stability of membranes used for the separation of industrial waste water polluted with hydrocarbons, the adhesion between the IP layer and the support layers has to be promoted.

4. Conclusions

Membranes used for water treatment often show a high instability and mechanical failure when traces of hydrocarbons are present in the water, making the use of cheap NF and RO membranes unsuitable for water treatment of industrial waste streams. We have shown that the stability of the thin film composite membrane is strongly dependent on the stability of the support material and the adhesion between the separating layer and the mechanical support. The polysulfone does not dissolve in water saturated with toluene, but instead a dewetting mechanism was observed. By improving the adhesion of the interfacial polymerization layer to the mechanical support, the dewetting of the IP film can be inhibited, allowing for a higher stability of the thin film composite membrane in industrial waste water streams containing traces of hydrocarbons. This would allow for the use of cheap and easy producible polysulfone supports for the use of industrial wastewater treatment membranes.

5. Acknowledgements

The authors would like to thank Bob Siemerink for his help with the FE-SEM pictures.

This work is part of the research programme *TA-ISPT Fundamentals* with project number 731.014.203, which is (partly) financed by the Netherlands Organisation for Scientific Research (NWO).

6. Data Availability

In addition to the data given in the Supplementary Information, the raw as well as the processed data required to reproduce these findings are available to download from DOI:10.4121/uuid:26b0fc62-3f0c-4391-9360-aafcd4861fc8.

7. References

[1] J.M. Neff, Preface, in: J.M. Neff (Ed.), Bioaccumulation Mar. Org., Elsevier, Oxford, 2002. doi:10.1016/B978-008043716-3/50000-2.

[2] S.D. Richardson, S.Y. Kimura, Water Analysis: Emerging Contaminants and Current Issues, Anal. Chem. 88 (2016) 546–582. doi:10.1021/acs.analchem.5b04493.

[3] A. Vengosh, R.B. Jackson, N. Warner, T.H. Darrah, A. Kondash, A Critical Review of the Risks to Water Resources from Unconventional Shale Gas Development and Hydraulic Fracturing in the United States, Environ. Sci. Technol. 48 (2014) 8334–8348. doi:10.1021/es405118y.

[4] S. Adham, A. Hussain, J. Minier-Matar, A. Janson, R. Sharma, Membrane applications and opportunities for water management in the oil & gas industry, Desalination. 440 (2018) 2–17. doi:10.1016/J.DESAL.2018.01.030.

[5] S. Munirasu, M.A. Haija, F. Banat, Use of membrane technology for oil field and refinery produced water treatment—A review, Process Saf. Environ. Prot. 100 (2016) 183–202. doi:10.1016/J.PSEP.2016.01.010.

[6] L.F. Greenlee, D.F. Lawler, B.D. Freeman, B. Marrot, P. Moulin, Reverse osmosis desalination: Water sources, technology, and today's challenges, Water Res. 43 (2009) 2317–2348. doi:10.1016/J.WATRES.2009.03.010.

[7] R.W. Baker, Membrane Technology and Applications, 3rd ed., John Wiley & Sons. Ltd., 2012.

[8] B. Van der Bruggen, C. Vandecasteele, Removal of pollutants from surface water and groundwater by nanofiltration: overview of possible applications in the drinking water industry, Environ. Pollut. 122 (2003) 435–445. doi:10.1016/S0269-7491(02)00308-1.

[9] M. Padaki, R. Surya Murali, M.S. Abdullah, N. Misdan, A. Moslehyani, M.A. Kassim, N. Hilal, A.F. Ismail, Membrane technology enhancement in oil–water separation. A review, Desalination. 357 (2015) 197–207. doi:10.1016/J.DESAL.2014.11.023.

[10] P. Xu, J.E. Drewes, T.-U. Kim, C. Bellona, G. Amy, Effect of membrane fouling on transport of organic contaminants in NF/RO membrane applications, J. Memb. Sci. 279 (2006) 165–175. doi:10.1016/J.MEMSCI.2005.12.001.

[11] C. Bellona, J.E. Drewes, P. Xu, G. Amy, Factors affecting the rejection of organic solutes during

NF/RO treatment—a literature review, Water Res. 38 (2004) 2795–2809. doi:10.1016/J.WATRES.2004.03.034.

[12] W.L. Ang, D. Nordin, A.W. Mohammad, A. Benamor, N. Hilal, Effect of membrane performance including fouling on cost optimization in brackish water desalination process, Chem. Eng. Res. Des. 117 (2017) 401–413. doi:10.1016/J.CHERD.2016.10.041.

[13] L.D. Nghiem, S. Hawkes, Effects of membrane fouling on the nanofiltration of trace organic contaminants, Desalination. 236 (2009) 273–281. doi:10.1016/J.DESAL.2007.10.077.

[14] H. Mehdizadeh, K. Molaiee-Nejad, Y.C. Chong, Modeling of mass transport of aqueous solutions of multi-solute organics through reverse osmosis membranes in case of solute-membrane affinity Part 1. Model development and simulation, J. Memb. Sci. 267 (2005) 27–40. doi:10.1016/j.memsci.2005.03.059.

[15] E.-S. Kim, Y. Liu, M. Gamal El-Din, The effects of pretreatment on nanofiltration and reverse osmosis membrane filtration for desalination of oil sands process-affected water, Sep. Purif. Technol. 81 (2011) 418–428. doi:10.1016/J.SEPPUR.2011.08.016.

[16] K.O. Agenson, T. Urase, Change in membrane performance due to organic fouling in nanofiltration (NF)/reverse osmosis (RO) applications, Sep. Purif. Technol. 55 (2007) 147–156. doi:10.1016/J.SEPPUR.2006.11.010.

[17] B. Van der Bruggen, L. Braeken, C. Vandecasteele, Flux decline in nanofiltration due to adsorption of organic compounds, Sep. Purif. Technol. 29 (2002) 23–31. doi:10.1016/S1383-5866(01)00199-X.

[18] A. Sotto, J.M. Arsuaga, B. Van der Bruggen, Sorption of phenolic compounds on NF/RO membrane surfaces: Influence on membrane performance, Desalination. 309 (2013) 64–73. doi:10.1016/J.DESAL.2012.09.023.

[19] S. Mondal, S.R. Wickramasinghe, Produced water treatment by nanofiltration and reverse osmosis membranes, J. Memb. Sci. 322 (2008) 162–170. doi:10.1016/j.memsci.2008.05.039.

[20] R.J. Petersen, Composite reverse osmosis and nanofiltration membranes, J. Memb. Sci. 83 (1993) 81–150. doi:10.1016/0376-7388(93)80014-O.

[21] K.P. Lee, T.C. Arnot, D. Mattia, A review of reverse osmosis membrane materials for desalination—Development to date and future potential, J. Memb. Sci. 370 (2011) 1–22. doi:10.1016/J.MEMSCI.2010.12.036.

[22] G.Z. Ramon, M.C.Y. Wong, E.M.V. Hoek, Transport through composite membrane, part 1: Is there an optimal support membrane?, J. Memb. Sci. 415–416 (2012) 298–305. doi:10.1016/J.MEMSCI.2012.05.013.

[23] W.J. Lau, A.F. Ismail, N. Misdan, M.A. Kassim, A recent progress in thin film composite membrane: A review, Desalination. 287 (2012) 190–199. doi:10.1016/j.desal.2011.04.004.

[24] P. Silva, S. Han, A.G. Livingston, Solvent transport in organic solvent nanofiltration membranes, J. Memb. Sci. 262 (2005) 49–59. doi:10.1016/j.memsci.2005.03.052.

[25] S. Poulson, R. Harrington, J. Drever, The solubility of toluene in aqueous salt solutions, Talanta. 48 (1999) 633–641. doi:10.1016/S0039-9140(98)00292-6.

[26] W. Ogieglo, H. Wormeester, M. Wessling, N.E. Benes, Spectroscopic ellipsometry analysis of a thin film composite membrane consisting of polysulfone on a porous alpha-alumina support, ACS Appl Mater Interfaces. 4 (2012) 935–943. doi:10.1021/am2015958.

[27] H.N. Altalyan, B. Jones, J. Bradd, L.D. Nghiem, Y.M. Alyazichi, Removal of volatile organic compounds (VOCs) from groundwater by reverse osmosis and nanofiltration, J. Water Process Eng. 9 (2016) 9–21. doi:10.1016/J.JWPE.2015.11.010.

[28] A.M. Comerton, R.C. Andrews, D.M. Bagley, P. Yang, Membrane adsorption of endocrine disrupting compounds and pharmaceutically active compounds, J. Memb. Sci. 303 (2007) 267–277. doi:10.1016/J.MEMSCI.2007.07.025.

[29] M. Mänttäri, A. Pihlajamäki, M. Nyström, Comparison of nanofiltration and tight ultrafiltration membranes in the filtration of paper mill process water, Desalination. 149 (2002) 131–136. doi:10.1016/S0011-9164(02)00744-0.

[30] A.R.D. Verliefde, E.R. Cornelissen, S.G.J. Heijman, E.M.V. Hoek, G.L. Amy, B. van der Brugggen, J.C. van Dijk, Influence of Solute-Membrane Affinity on Rejection of Uncharged Organic Solutes by Nanofiltration Membranes, Environ. Sci. Technol. 43 (2009) 2400–2406. doi:10.1021/es803146r.

[31] I.C. Kim, J. Jegal, K.H. Lee, Effect of aqueous and organic solutions on the performance of polyamide thin-film-composite nanofiltration membranes, J. Polym. Sci. Part B Polym. Phys. 40 (2002) 2151–2163. doi:10.1002/polb.10265.

[32] S. Darvishmanesh, J.C. Jansen, F. Tasselli, E. Tocci, P. Luis, J. Degrève, E. Drioli, B. Van der Bruggen, Novel polyphenylsulfone membrane for potential use in solvent nanofiltration, J. Memb. Sci. 379 (2011) 60–68. doi:10.1016/J.MEMSCI.2011.05.045.

[33] L. Xue, Y. Han, Inhibition of dewetting of thin polymer films, Prog. Mater. Sci. 57 (2012) 947–979. doi:10.1016/j.pmatsci.2012.01.003.

[34] T.S. Chow, Molecular Interpretation of the Glass Transition Temperature of Polymer-Diluent systems, Macromolecules. 13 (1980) 362–364. doi:10.1021/ma60074a029.

[35] K. Hermansson, U. Lindberg, B. Hok, G. Palmskog, Wetting properties of silicon surfaces, in: TRANSDUCERS '91 1991 Int. Conf. Solid-State Sensors Actuators. Dig. Tech. Pap., 1991: pp. 193–196. doi:10.1109/SENSOR.1991.148835.

[36] E. Bormashenko, R. Pogreb, G. Whyman, Y. Bormashenko, R. Jager, T. Stein, A. Schechter, D. Aurbach, The Reversible Giant Change in the Contact Angle on the Polysulfone and Polyethersulfone Films Exposed to UV Irradiation, Langmuir. 24 (2008) 5977–5980. doi:10.1021/la800527q.

[37] V. Altun, Solvent stable UV and EB cross-linked polysulfone based membranes, 2016.